URSI GASS 2020, Rome, Italy, 29 August - 5 September 2020

Development of high-performance Q-band waveguide assemblies for polarization measurements

Oscar Antonio Peverini (1), Giuseppe Virone (1), Giuseppe Addamo (1), Mauro Lumia (1), Fabio Paonessa(1), Aniello Mennella (2), Marco Bersanelli (2), Cristian Franceschet (2), Mario Zannoni (3)

(1) IEIIT-CNR, c/o Politecnico di Torino, C.so Duca degli Abruzzi 24, 10129 Torino, Italy,
Email: oscar.peverini@ieiit.cnr.it
(2) Dipartimento di Fisica, Università degli Studi di Milano, via Celoria, 16, 20133 Milano, Italy
(3) Dipartimento di Fisica, Università di Milano - Bicocca, P.zza della Scienza 3, 20126 Milano, Italy

Abstract

This paper reports on the Q-band antenna feed chains developed for the STRIP coherent multi-feed instrument of the Large Scale Polarization Explorer. The array elements are arranged in a honeycomb lattice of seven hexagonal modules, each including seven feed-horns. Each 7-elements module is built with the platelet technique. A split-block design of groove polarizers and an ad-hoc assembly procedure have been conceived in order to achieve recurring high-performance for all the 49 polarizers (i.e., cross-polarization < -35 dB, return-loss > 36 dB, insertion-loss < 0.07 dB). The ortho-mode transducers are based on a novel multi-layer turnstile-junction design. This configuration has been conceived toward a high parallelization rate of the manufacturing process, while providing high electromagnetic performance (cross-coupling < -50 dB, isolation > 50 dB).

1. Introduction

The Large Scale Polarization Explorer (LSPE) is a project funded by the Italian Space Agency and the National Institute for Nuclear Physics (INFN) that combines ground-based (STRIP) and balloon-borne (SWIPE) polarization measurements of the microwave sky on large angular scales to attempt a detection of the B-modes of the Cosmic Microwave Background (CMB) polarization. STRIP [1] will observe approximately 25% of the Northern sky from the “Observatorio del Teide” in Tenerife, using coherent polarimeters operating in the Q-band. This instrument is based on the simultaneous detection of the Q and U Stokes parameters of the incoming radiation through an array of forty-nine correlation receivers operating from 39 GHz to 48 GHz (20% bandwidth). The receiver array will consist of 7 hexagonal modules, each containing seven receivers elements (see Figure 1), placed in the focal plane of a 1.5 m Dragonian side-fed dual reflector telescope and will be enclosed in a cryostat cooled to 20K by a pulsed tube cooler. A second frequency channel with six-elements at 95 GHz will be exploited as an atmospheric monitor.

2. LSPE-STRIP receiver architecture

The operation of each receiver is based on the measurement of the correlation between the Right- and Left-Hand Circular Polarization (RHCP and LHCP) components of the electromagnetic signal. The schematic of the receiver architecture is shown in Figure 2. The RHCP and LHCP components (labelled A and B, respectively) are collected through the corrugated horn and routed to the polarizer [2]. The latter converts the two circular polarizations in two linearly polarized signals oriented along the main axes of the ortho-mode transducer (OMT) [3]. To this aim, the polarizer principal-axes L and C are rotated by 45 deg with respect to the OMT axes. The two linearly polarized signals are, hence, separated in the common waveguide through the OMT and, subsequently, routed to the correlation unit. This is a Monolithic Microwave Integrated Circuit (MMIC) based on the design developed for the QUIET experiment [4]. According to the layout reported in [1], the correlation unit integrates six low-noise HEMT amplifiers, two-phase switches, a 180-deg hybrid coupler, two power-splitters, four band-pass filters, a 90-deg hybrid coupler and four diode detectors. The chip provides four output voltages that are proportional to the sum and difference, in phase and in quadrature, of the input RF signals A and B. The same architecture, but with a waveguide correlation unit is described in [5].

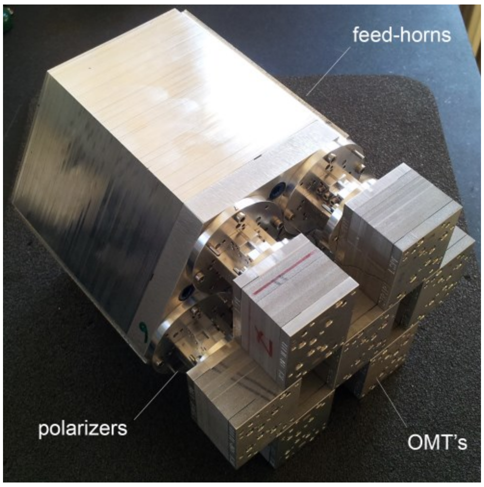

Figure 1. Q-band hexagonal antenna-feed module.

In order to identify the best polarizer and ortho-mode transducer designs for the LSPE-STRIP correlation receivers, the electromagnetic behavior of these components have been described in terms of the Muller matrix $\boldsymbol{M}$ relating the input and output Stoke parameters:

$$\begin{bmatrix} Q \\ U \\ V \\ I \end{bmatrix}_{\mathbf{out}} = \boldsymbol{M} \cdot \begin{bmatrix} Q \\ U \\ V \\ I \end{bmatrix}_{\mathbf{in}} = \begin{bmatrix} \boldsymbol{H} & \boldsymbol{K} \\ \boldsymbol{P} & \boldsymbol{N} \end{bmatrix} \cdot \begin{bmatrix} Q \\ U \\ V \\ I \end{bmatrix}_{\mathbf{in}} .$$

Since the goal of the LSPE-STRIP instrument is the measurement of the Q and U Stokes parameters, the relevant blocks of the Muller matrix are the sub-matrices $\boldsymbol{H}$ and $\boldsymbol{K}$ defining the relationship:

$$\begin{bmatrix} Q \\ U \end{bmatrix}_{\text{out}} = \begin{bmatrix} H_{QQ} & H_{QU} \\ H_{UQ} & H_{UU} \end{bmatrix} \cdot \begin{bmatrix} Q \\ U \end{bmatrix}_{\text{in}} + \begin{bmatrix} K_{QV} & K_{QI} \\ K_{UV} & K_{UI} \end{bmatrix} \cdot \begin{bmatrix} V \\ I \end{bmatrix}_{\text{in}} .$$

The most demanding requirements set on the LSPE-STRIP receivers involve the coefficients K_{QI} and K_{UI} that define the spurious leakage of the total intensity I in the Q and U channels. Indeed, I contains both the polarized and unpolarised CMB components and, hence, it is several orders of magnitude larger than the Q and U components to be detected.

The following sections reports the modelling, design and experimental characterization of the Q-band feed-horns, polarizer and OMT modules developed for the LSPE-STRIP.

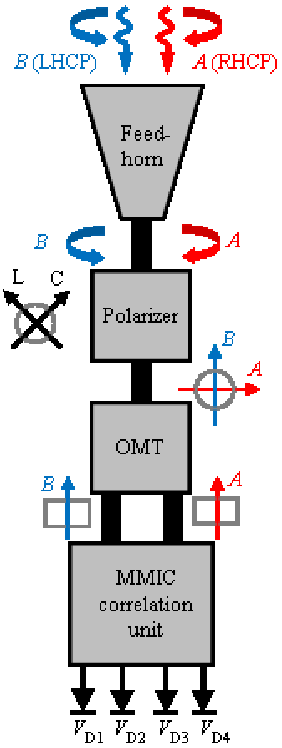

Figure 2. Schematic of the Q-band dual-polarization correlation receiver of the LSPE-STRIP instrument. L and C denote the inductive and capacitive principal polarizer axes.

3. Feed-horns array

The first element of each radiometric chain is a corrugated feed-horn which guarantees optimal performance in terms of beam symmetry, cross-polar response and sidelobes level. Each feed-horn is based on a dual-profiled design with a $\sin^2$ section followed by an exponential section up to the aperture, giving the best compromise between performances and compactness. The 49 Q-band feed-horns are arranged in a honeycomb lattice of seven hexagonal modules, each including seven feed-horns. Each 7-elements module is built with the platelet technique (see [6], [7]) which allows us to build the horn by stacking aluminum plates, each one containing a tooth and a groove of each corrugation.

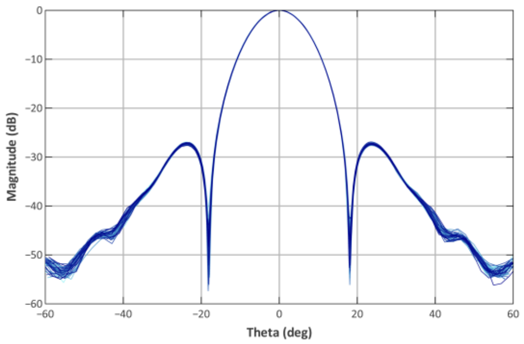

Figure 3. Measured radiation pattern in the co-polar E-plane of all 49 feed-horns at 43 GHz. Simulation is also reported in the plot (black line)

The radiation patterns of all feed-horns have been measured at selected frequencies in the Q-band. They resulted highly consistent with each other and in agreement with the simulations within fractions of a dB up to the first side-lobe, as shown in Figure 3. Cross-polarization and return loss levels are better than -37 dB and 40 dB, respectively, on the whole 39-48 GHz frequency band.

The modelling of the radiation pattern of the feed-horn when coupled to a dual circular polarization system is also reported in [8].

4. Polarizers

The elements of the matrices $\boldsymbol{H}$ and $\boldsymbol{K}$ are derived as a function of the matrix transmission coefficients $\boldsymbol{T}$ of the polarizers:

$$H_{QQ} = \frac{1}{2}\{|T_{\text{LL}}|^2 + |T_{\text{CC}}|^2\}$$

$$H_{QU} = H_{UQ} = 0$$

$$H_{UU} = \text{Im}\{T_{\text{LL}} T_{\text{CC}}^*\}$$

$$K_{QI} = \frac{1}{2}\{|T_{\text{LL}}|^2 - |T_{\text{CC}}|^2\}$$

$$K_{QV} = K_{UI} = 0$$

$$K_{UV} = \text{-Re}\{T_{\mathrm{LL}} T_{\mathrm{CC}}^{*}\}.$$

where L and C denote the inductive and capacitive principal polarizer axes. From these equations, it can be easily inferred that any deviation of the phase difference between the two principal-polarization transmission coefficients from theoretical value of 90 deg leads to a loss in the detected U parameter and a leakage of the Stoke parameter V in the U channel. Even more essential is the minimization of the insertion loss difference between the two principal-polarization transmissions, since it leads to a total intensity leakage in the Q channel.

In order to meet the aforesaid requirements at affordable costs, a groove polarizer based on a split-block layout has been designed. All the grooves are realized in two comb plates [9] of constant thickness. The depth of the grooves and the height of the waveguide ridges between the grooves have been defined according to an optimum-set procedure similar to that reported in [10]-[11].

The analysis has been carried out exploiting an in-house spectral element-code [12]. The polarizer consists of six mechanical parts that have been accurately aligned through an ad-hoc assembling procedure based on the use of Johansson gauges. This procedure has also allowed us to fine-tune the comb plates in order to compensate for the manufacturing uncertainties (< 0.02 mm). Two prototypes with different comb plate thickness (1.5 and 3.0 mm) have previously been machined and tested. Subsequently, on the basis of the selected layout, all the 49 operational units have been manufactured and tested at room temperature in the principal-polarization basis.

The measurements of the 49 Q-band polarizers show a return loss better than 36 dB, with an insertion loss lower than 0.07 dB, a phase difference deviation from 90 deg lower than 2 deg which corresponds to a cross-polarization lower than -35 dB. The insertion loss unbalancing is lower than 0.01 dB.

The second column of Tab.1 reports the corresponding measured values of the blocks $\boldsymbol{H}$ and $\boldsymbol{K}$. It has to be remarked that the total intensity leakage in the Q channel (K_{QI}) is lower than -25 dB in the working band.

5. Ortho-mode Transducers

The elements of the Muller matrix have been derived as a function of the OMT transmission matrix components $\boldsymbol{T}$:

$$H_{QQ} = \text{Re}\{T_{AA}T_{BB}^{*} + T_{AB}T_{BA}^{*}\}$$

$$H_{QU} = -\,\text{Im}\{T_{AA}T_{BB}^{*} - T_{AB}T_{BA}^{*}\}$$

$$H_{UQ} = \text{Im}\{T_{AA}T_{BB}^{*} + T_{AB}T_{BA}^{*}\}$$

$$H_{UU} = \text{Re}\{T_{AA}T_{BB}^{*} - T_{AB}T_{BA}^{*}\}$$

and

$$K_{QI} = \text{Re}\{T_{AA}T_{BA}^{*} + T_{AB}T_{BB}^{*}\}$$

$$K_{QV} = \text{-Re}\{T_{AA}T_{BA}^{*} - T_{AB}T_{BB}^{*}\}$$

$$K_{UI} = \text{Im}\{T_{AA}T_{BA}^{*} + T_{AB}T_{BB}^{*}\}$$

$$K_{UV} = -\text{Im}\{T_{AA}T_{BA}^{*} - T_{AB}T_{BB}^{*}\}.$$

Since the block $\boldsymbol{H}$ has to be as close as possible to the identity matrix, the OMT cross-polar transmission coefficients (T_{AB} and T_{BA}) should be minimized, and the two co-polar transmission coefficients (T_{AA} and T_{BB}) should be phase-equalized. Under these conditions, the spurious contamination matrix $\boldsymbol{K}$ is also minimized. However, it has to be noticed that the total intensity leakage terms (K_{QI} and K_{UI}) affecting the *Q* and *U* OMT channels depend on the term

$$T_{AA}T_{BA}^{*} + T_{AB}T_{BB}^{*}.$$

It can be easily proved that this quantity is ideally zero for a perfectly-matched loss-less OMT. Hence, high values of OMT return-loss reduce the spurious contamination due to the total intensity.

Based on these electromagnetic requirements, the turnstile-junction symmetric OMT, reported in details in [13], has been designed. This configuration is particularly suitable for the medium-scale production of high-performance OMTs used in multi-feed dual-polarization instrumentation aimed at astrophysical and radio-astronomical surveys. Indeed, only standard-thickness Al plates have been used, and wire electrical-discharge machining (EDM) of stacks consisting of identical plates has allowed for manufacturing parallelization. In order to identify the best material, the electrical resistivity of different standard-thickness metal layers has been measured both at room- and at cryogenic temperature. A similar approach has been exploited for the development of W-band cluster instrumentation [14]. On the basis of the select Al-alloy, five OMT prototypes have been preliminarily manufactured and tested. In particular, the prototypes have undergone thermal cycles down to 15 K in order to assess their compliance to operation in cryogenic environment. Subsequently, all the 49 OMT flight units have been developed and measured through the full dual-polarization procedure reported in [15].

Additionally the co-polar transmission coefficients have been measured by exploiting the technique reported in [16], since the balancing between the two polarization channels is an import parameter for the application. The measured return loss is better than 22 dB with an insertion-loss lower than 0.7 dB and isolation and cross-couplings better than 40 dB and -35 dB, respectively. The third column of Tab. 1 reports the measured coefficients of the Muller matrix blocks $\boldsymbol{H}$ and $\boldsymbol{K}$. It can be noticed that levels lower than approximately -30 dB have been achieved for spurious leakage coefficients K_{QI} and K_{UI}.

	Polarizer	**OMT**	**Polarizers + OMTs sub-assemblies**
Sub-matrix $\boldsymbol{H}$			
H_{QQ}	≥ -0.06 dB	≥ -0.6 dB	≥ -0.7 dB
H_{QU}	-	≤ -15 dB	≤ -14 dB ≤-20 dB with shim and post-processing
H_{UQ}	-	≤ -15 dB	≤ -14 dB ≤-20 dB with shim and post-processing
H_{UU}	≥ -0.06 dB	≥ -0.6 dB	≥ -0.7 dB
Sub-matrix $\boldsymbol{K}$			
K_{QV}	-	≤ -28 dB	≤ -17 dB
K_{QI}	≤ -25 dB	≤ -29 dB	≤ -25 dB
K_{UV}	≤ -15 dB	≤ -23 dB	≤ -15 dB
K_{UI}	-	≤ -30 dB	≤ -30 dB

Table 1. Measured coefficients of the blocks H and K of the Mueller matrix.

6. Polarizers and Ortho-Mode Transducers sub-assemblies

The 49 Q-band sub-assemblies, each consisting of polarizers and OMTs, have been mounted and measured at room temperature. The fourth column in Table 1 reports all the coefficients of the sub-matrices $\boldsymbol{H}$ and $\boldsymbol{K}$. The rejection levels to the total intensity I is approximately 25 dB and 30 dB for the Q and U channels, respectively. The values of the coefficients K_{QV} and K_{UV} are instead in the order of -15 dB. Since the Stokes parameters are quadratic quantities, the values of K_{QV} and K_{UV} are commensurate with the cross-coupling levels of approximately -35 dB that are provided by the sub-assemblies (mainly by the polarizers). The lower values of the coefficients K_{QI} and K_{UI} arise from an adequate fulfilment of the loss-less and matching condition. It has also to be remarked that the off-diagonal entries of matrix $\boldsymbol{H}$ can be minimized through a befitting shimming (in the order of 0.01-0.05 mm) of the output WR22 ports and through an off-line rotation of the detected coefficients in the Q - U plane.

7. Acknowledgements

This work has been carried out in the context of the ASI program “Large Scale Polarization Experiment (LSPE)” (contract I/022/11/0).

8. References

1. C. Franceschet, et al., “The STRIP instrument of the Large Scale Polarization Explorer: microwave eyes to map the Galactic polarized foregrounds”, in Proc. of the SPIE Conference Astronomical Telescopes + Instrumentation 2018, Austin, Texas, July 2018.
2. J. Boremann et al., “Analysis and design of circular ridged waveguide components”, IEEE Trans. on Microw. Theory Tech., vol. 47, no. 3, pp. 330-335, Mar 1999.
3. J. Uher, J. Bornemann, and U. Rosenberg, “Waveguide Components for Antenna Feed Systems”: Theory and CAD. Norwood, MA, USA:Artech House, 1993.
4. QUIET Collaboration, “The Q/U imaging experiment instrument”, The Astrophysical Journal, vol. 768, no 1, May 2013.
5. Cortiglioni S., “BaR-SPOrt: An experiment to measure the linearly polarized sky emission from both the cosmic microwave background and foregrounds”, in 16th ESA Symposium on European Rocket and Balloon Programmes and Related Research, 2 - 5 June 2003.
6. Del Torto, F., et al., “W-band prototype of platelet feed-horn array for CMB polarisation measurements”, Journal of Instrumentation 6(06), P06009 (2011).
7. Del Torto, F., Franceschet, C., et al. “A 7x7 elements Q-band feed-horn array for the LSPE-STRIP experiment”, Proc. 36th ESA Antenna Workshop on Antennas and RF Systems for Space Science (2015).
8. Realini, S., et al, “Modelling the radiation pattern of a dual circular polarization system”, 2019 JINST 14 P03005
9. S. Y. Eom, and Y. B. Korchemkin, “A New comb circular polarizer suitable for millimeter-band application”, ETRI Journal, vol. 28, no. 5, pp. 656-659, Oct. 2006.
10. G. Virone, et al., “Optimum-Iris-Set Concept for Waveguide Polarizers”, IEEE Microwave and Wireless Components Letters, vol. 17, no. 3, pp. 202-204, March 2007.
11. G. Virone et al. “Combined-phase-shift waveguide polarizer”, IEEE Microwave and Wireless Components Letters, vol. 18, no. 8, pp. 509-511, Aug. 2008.
12. O.A. Peverini et al. “A spectral-element method for the analysis of 2-D waveguide devices with sharp edges and irregular shapes”, IEEE Trans. on Microw. Theory Tech., vol. 59, no. 7, pp. 1685 -1695, July 2011.
13. G. Virone, et al., “Platelet orthomode transducer for Q-band correlation polarimeter clusters”, IEEE Trans. on Microw. Theory Techn., vol. 62, no. 7, pp.1487-1493, July 2014.
14. G. Virone et al. “W-band orthomode transducer for dense focal-plane clusters”, IEEE Microwave and Wireless Components Letters, vol. 25, no. 2, pp. 85-87, Feb. 2015.
15. O. A. Peverini, et al., “A Microwave measurement procedure for a full characterization of ortho-mode transducers”, IEEE Trans. on Microw. Theory Tech., vol. 51, no. 4, pp. 1207 -1213, April 2003.
16. O.A. Peverini et al., “A hybrid TSD-RSOL technique for the measurement of non-insertable devices”, ICEAA 2011.